MECSOL 2022 - Proceedings of the 8th International Symposium on Solid Mechanics
M.L. Bittencourt, J. Labaki, L.C.M. Vieira Jr. and E. Mesquita (Editors), Campinas SP, Brazil, October 17th to 19th, 2022

Numerical and experimental study of ductile fracture using specimens in asymmetric four-point bending

Daniel López Giraldo [1], Diego F. B. Sarzosa [1]

[1] Department of Naval Architecture and Ocean Engineering, University of São Paulo, São Paulo, Brazil
danilopgi@usp.br dsarzosa@usp.br

Abstract: The experimental determination of the fracture toughness of ductile materials under load mode I, based on the behavior of the J-integral, was extensively formalized in ASTM E 1820-18 and in ESIS procedure P1-92. However, regarding to combined loading modes, generally accepted rules for the evaluation of fracture toughness are still lacking, despite their importance in many engineering situations. It is known that the measurement of fracture toughness based on the J-integral is highly dependent on the combined loading mode, the geometry of the tested sample and the general state of strain/stress of the crack-tip sample. This research consists of the development of an experimental protocol for the four-point asymmetric bending test, by means of which it is possible to study the response to fracture of metallic materials under combined loading modes. The reliability of the results will be evaluated by comparing experimental and computational tests with different settings of the experimental and numerical studies. Numerical analyses using the finite element method are performed to define the test conditions and characterize the mechanical response of the material. The preliminary results are favorable to the proposed methodology, presenting consistency between computational results and experimental results presented in the open literature.

Keywords: fracture, tenacity, bending, asymmetry, finite elements.

INTRODUCTION

It is very important that in critical engineering structures - such as pressure vessels, offshore/onshore pipelines, and others - an adequate characterization of the fracture toughness is carried out. Depending on the possible loads applied on the structure, different fracture modes can occur. For example, bending and torsional moments will generate different modes of crack opening in cracked components. There are numerous studies on Fracture Mechanics directed at a single loading mode, however, regarding combined loading modes, there is still much to study. One of the recently introduced methods for the study of cracked bodies under combined loading modes is the AFPB (Asymmetric Four-Point Bending test) which was initially introduced by Arrea and Ingraffea (1986). This test generates opening (mode I) and shear (mode II) load modes on the crack plane. Thanks to the investigations that have been carried out around the AFPB test, there are already expressions to calculate the J-integral (Tohgo and Ishii, 1992) and the Stress Intensity Factor (He and Hutchinson, 2000). These expressions are very useful when developing numerical models intended to replicate experimental tests, with the aim of obtaining a greater number of results for various test configurations.

Motivated by the importance of considering the combined load modes in cracked body studies, this study will focus on the design of finite element models, using the ABAQUS software, for the recovery of J-integral values in asymmetric four-points bending tests.

EXPERIMENTAL TESTS

This section provides details of the experimental tests used in the present study, conducted by Qian and Yang (2012). The data used as input for the numerical models are presented in this section. That study investigates the effect of combined loading modes on the initiation of ductile crack extensions for aluminum alloy 5083-H112. This investigation is appropriate because the numerical models developed in the present study do not contain a damage model and therefore will not present tearing. Then, it will only be possible to calculate the J-integral up to the moment of crack propagation initiation.

Figure 1 below shows the geometry of the bodies used, where c corresponds to the distance between the applied loading point (P) and the crack plane, b_1 represents the distance between the loading point and its nearest support, a is the crack depth, B is the specimen thickness and W is the specimen width. The variation of the distance c generates different combined loading modes at the crack tip. The distance b_1 was fixed at $b_1 = 40$ mm and the distance b_2 at $b_2 = 2b_1$. Table 1 presents the different test configurations used in this study.

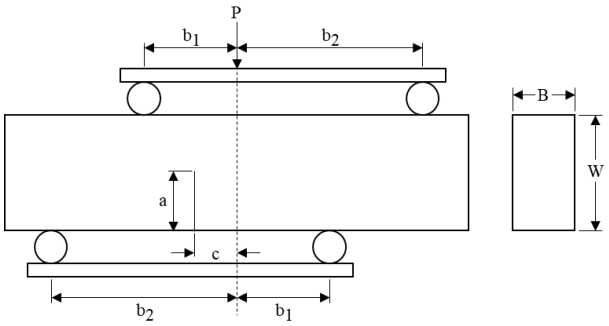

Figure 1 – Specimen geometry and test parameters.

Table 1 – Summary of the mixed-mode specimens.

Specimen name	a_0 (mm)	a_0/W	c (mm)	B (mm)
M1	18.6	0.517	20	
M3	18.7	0.518	5	18.2
M6	18.9	0.526	0	

Mechanical Properties of Material

The mechanical properties of the aluminum alloy 5083-H112 were obtained from the work of Qian and Yang (2012). They performed tensile tests at room temperature, following the guidelines of the ASTM E8M-04 standard (2004). Figure 2 presents the engineering stress versus engineering strain curve and the true stress versus true strain curve measured from coupon specimens with the thickness equal to 15 mm. The solid circle in the Fig. 2 indicates the true stress computed from the maximum engineering stress. Other mechanical properties of the material include Young's modulus E = 69 GPa, Poisson's ratio $\nu = 0.35$, yield stress $\sigma_y = 243$ MPa and ultimate stress $\sigma_u = 347$ MPa. Mechanical properties were used as inputs for numerical analyses.

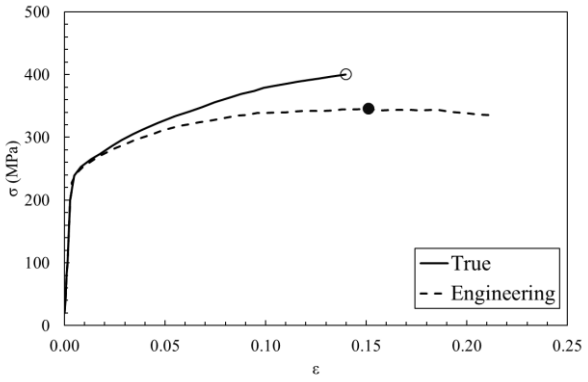

Figure 2 – Stress-strain relationships for the aluminum alloy 5083-H112.

J-value for mixed-mode I and II specimens

Tohgo and Ishii (1992) proposed a method to determine J-integral values for the four-point asymmetric bending test by measuring the local deformation at the crack plane. They separated the total energy release rate, J_T, into:

$$J_T = J_I + J_{II} \tag{1}$$

Where J_I is the opening-mode energy release rate and J_{II} corresponds to the shear-mode energy release.

$$J_I = \frac{2}{bB}\int_0^{\theta} M d\theta \tag{2}$$

$$J_{II} = J_{II}^{e} + \frac{2}{bB}\left[\int_0^{\delta_V} F_V d\delta \; - \; \frac{1}{2} F \delta_V\right] \tag{3}$$

Where b denotes the length of the remaining ligament, M and F_V refers to the bending moment and the shear force applied at the crack plane respectively, θ is the rotation between two crack planes and δ_V represents the shear displacement between the two crack planes. The elastic J_{II}^e follows:

$$J_{II}^e = \frac{K_{II}^2(1 - \nu^2)}{E} \tag{4}$$

Where K_{II} denotes the mode II stress-intensity factor determined form finite elements results and ν and E corresponds to the Poisson's ratio and Young's modulus respectively. Figure 3 illustrates schematically the deformed crack tip under mixed-mode I and II loading.

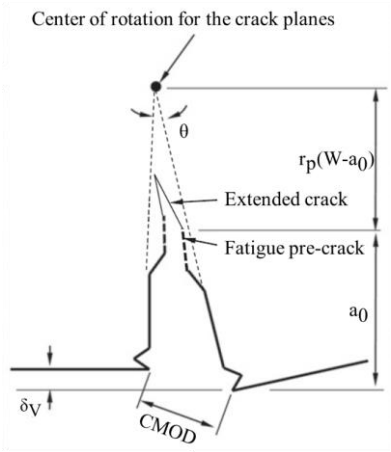

Figure 3 – Crack tip deformed under mixed mode I and II loading.

To obtain the value of θ, Tohgo and Ishii (1992) propose,

$$\theta = \frac{CMOD}{a_0 + r_p(W - a_0)} \tag{5}$$

Where r_p represents the plastic rotation factor and equals to 0.44 as suggested in ASTM E1820 (2011) for bending specimens. To calculate the bending moment and the shear force acting on the crack plane, it is enough to carry out a simple static load analysis to obtain,

$$F_V = \frac{b_2 - b_1}{b_2 + b_1} P \tag{6}$$

$$M = cF_V \tag{7}$$

Finally, Hallback and Nilsson () define the equivalent mode-mixite angle as,

$$\beta_{eq} = \tan^{-1}(K_I/K_{II}) \tag{8}$$

Where β_{eq}=90° represents the pure mode I loading and β_{eq}=0° corresponds to the pure mode II loading. F_V (mm)

Experimental Results

The experimental results obtained by Qian and Yang (2012) are presented in this section. These results were obtained following the guidelines recommended by Tohgo and Ishii (1992). The loading procedure includes a displacement-controlled load applied at 0.1 mm/min, with multiple unloading–reloading cycles to monitor the change in the specimen's compliance as the crack extends. All specimens were tested at room temperature (T = 25°). Figures 4a and 4b show the F_V-δ_V and M-θ curves respectively, measured for the tree samples studied. The solid circles represent the values reported as the start of crack propagation and on these points the J-integral was calculated. Table 2 presents the results of the J-integral.

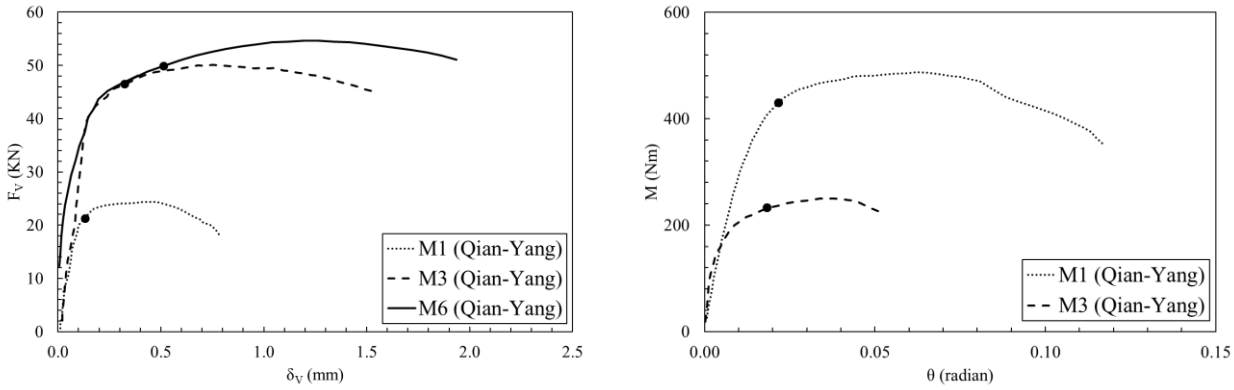

(a) (b)

Figure 3 – (a) F_V-δ_V curve and (b) M-θ curve.

Table 2 – J-integral results and the local crack-plane deformation.

Specimen	β_{eq} (°)	J_I (KJ/m^2)	J_{II} (KJ/m^2)	J_T (KJ/m^2)	δ_V (mm)	CMOD (mm)	P (KN)
M1	75	43.7	3.0	46.7	0.13	0.57	64
M3	45	23.2	29.6	52.8	0.32	0.48	138
M6	0	0.0	61.3	61.3	0.50	0.00	150

3D FINITE ELEMENT MODEL

Finite element models were constructed, according to the nominal dimensions of the specimens used in the experimental tests (table 1), to recover the F_V-δ_V and M-θ curves, and the J-integral results. In the present study, the numerical simulations were made using the ABAQUS software – which has proven to be an effective way to studying the ductile fracture mechanism (Zhang et al. 2014).

A schematic of the model as well as the applied boundary and mesh conditions are shown in Fig. 5 below. In the region around the crack, a relatively finer spider mesh was applied. At the tip of the crack, a mesh with linear 6-node triangular prism elements (C3D6) was applied. And a mesh with 8-node linear block elements (C3D8R) was applied to the other elements of the model.

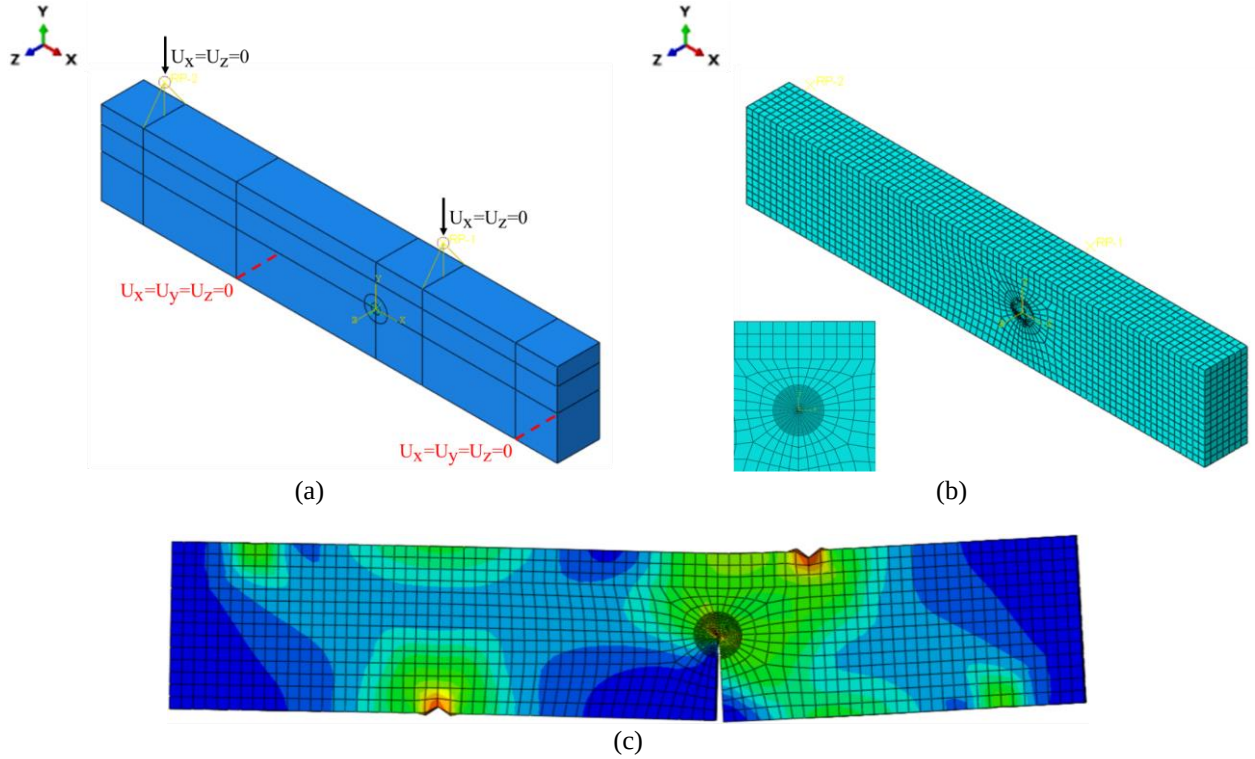

(a) (b)

(c)

Figure 4 – (a) boundary conditions applied, (b) mesh used and (c) deformed numerical model.

Numerical Results

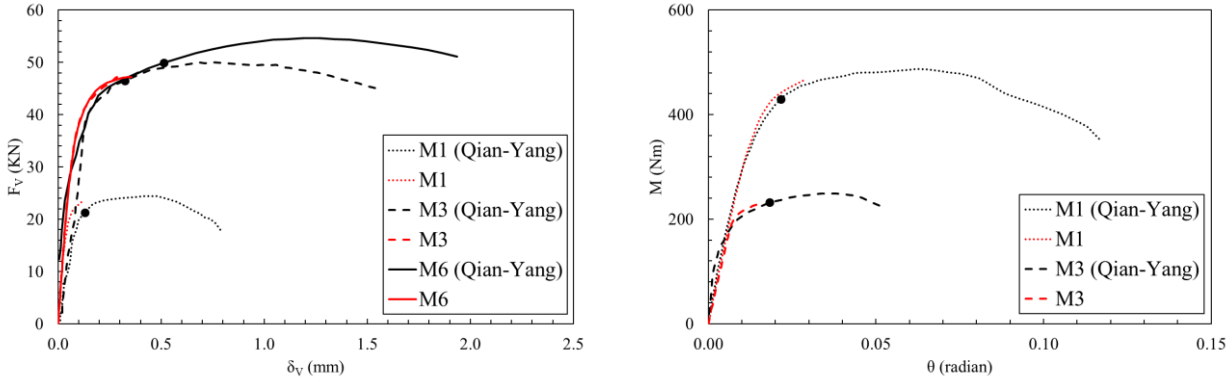

(a) (b)

Figure 5 – (a) F_V-δ_V curve and (b) M-θ curve.

Table 3 – J-integral results and the local crack-plane deformation.

Specimen	β_{eq} (°)	J_I (KJ/m^2)	J_{II} (KJ/m^2)	J_T (KJ/m^2)	δ_V (mm)	CMOD (mm)	P (KN)
M1 (Qian-Yang)	75.0	43.7	3.0	46.7	0.13	0.57	64.0
M1	74.8	42.2	4.2	46.5	0.09	0.61	67.2
M3 (Qian-Yang)	45.0	23.2	29.6	52.8	0.32	0.48	138.0
M3	42.7	16.6	31.5	48.1	0.29	0.42	141.6
M6 (Qian-Yang)	0.0	0.0	61.3	61.3	0.50	0.00	150.0
M6	0.0	0.0	65.2	65.2	0.51	0.52	175.0

Comparison of results

The developed model showed a good adherence in the response of the F_V-δ_V and M-θ curves with respect to the experimental results. The numerical results do not completely cover the experimental results, because the numerical model does not have a damage model. This indicates that the model will only reach the maximum possible strain, then it will stop just at the moment of crack propagation. Under this same argument, the small difference observed between the F_V-δ_V curves of specimen M1 can be justified.

With respect to the calculations of the J-integral, the results are relatively accurate. However, regarding the auxiliary parameters that characterize the local crack-plane deformation, the results are not very accurate. This can be justified by the lack of a damage model thus the numerical model will present a greater deformation at the time of crack propagation.

Conclusions

In the present study, the recovery of the F_V-δ_V and M-θ curves of specimens under the four-point asymmetric bending test, with different eccentricity configurations and with deep crack depth, was evaluated. Subsequently, the values of the J-integral were calculated. In the end, the model presented results close to those expected, which shows that the use of numerical models is reasonable to represent the evolution of ductile fracture.

ACKNOWLEDGMENTS

This study is supported by the Foundation for the Technological Development of Engineering (FDTE) and the Department of Naval and Oceanic Engineering at the University of São Paulo.

REFERENCES

Arrea M. and Ingraffea J.W., 1982, “Mixed Mode Crack Propagation in Mortar and Concrete”, Cornell University, Ithaca.

ASTM, 2011, “Standard test method for measurement of fracture toughness”, E1820-11, West Conshohocken.

ASTM, 2004, “Standard test methods for tension testing of metallic materials”, E8M-04.

Hallback N, Nilsson F., 1994, “Mixed-mode I/II fracture behavior of an aluminum-alloy”, J Mech Phys Solids, vol. 42(9), pp. 1345-74.

Qian X. and Yang W., 2012, “Initiation of ductile fracture in mixed-mode I and II aluminum alloy specimens”, Engineering Fracture Mechanics, vol. 93, pp. 189-203.

Tohgo K. and Ishii H., 1992, “Elastic-plastic fracture toughness test under mixed mode I-II loading”, Engineering Fracture Mechanics, vol. 41, pp. 529-540.

Zhang B., Ye C., Liang B., et al., 2014, “Ductile failure analysis and crack behavior of X65 buried pipes using extended finite element method”, Engineering Failure Analysis, vol. 45(8), pp. 26-40.